

## EVALUATION OF INTERFACE FAILURE THROUGH DIGITAL IMAGE CORRELATION INVESTIGATIONS

Matei Constantin MIRON<sup>1</sup>, Dan Mihai CONSTANTINESCU<sup>2</sup>

*Metoda corelării digitale a imaginii este folosită pentru descrierea fenomenelor de degradare interlaminară și de cedare a zonei de interfață, specifice materialelor de tip sandwich.*

*Testele realizate prin încărcarea în modul I a zonei de interfață oferă rezultate interesante legate de localizarea degradării și a variației deformațiilor specifice la finalizarea degradării. În urma analizei experimentale se fac observații cu privire la existența a patru domenii principale ce descriu deformațiile specifice ce iau naștere în zona de interfață și în miezul materialului. Deschiderea fisurii poate fi măsurată în momentul finalizării degradării, respectiv în momentul în care fisura se propagă.*

*Interface damage characterization and interlaminar failure of sandwich specimens with one initial interlaminar delamination is done by using the digital image correlation method.*

*Mode I tests reveal interesting particularities on damage localization and strain variation when damage is finalized. After analyzing the experimentally obtained results, we make comments on the four characteristic domains which describe the opening strains in the interface and in the core. The crack opening can be also measured when damage is finalized and crack grows further on.*

**Keywords:** interlaminar failure, digital image correlation, crack propagation, sandwich composite

### 1. Introduction

The laminated and sandwich composite material concept has a huge potential and special attention should be given to possible structural collapse which is often caused by the evolution of different types of damages created in a local zone of the structure. The particular damage modes depend upon loading, lay-up and stacking sequence. For a laminated or sandwich composite material it is essential to understand and control its lay-ups arrangement for special orthotropy, the laminate design, strain and stress analysis, stiffness, and failure

<sup>1</sup> PhD Student, Department of Strength of Materials, University POLITEHNICA of Bucharest, Romania, e-mail: matei.miron@yahoo.com

<sup>2</sup> Professor, Department of Strength of Materials, University POLITEHNICA of Bucharest, Romania, e-mail: dan.constantinescu@upb.ro

characterization, that is: failure modes and analysis, failure criteria, and edge delamination problems.

The fracture behaviour of high performance composite laminates is a complex issue, involving both intralaminar damage mechanisms (e.g. matrix cracking, fibre breaking) and interlaminar damage (delamination). Some progress has been made lately in the development of analytical tools for the prediction of intralaminar damage growth, but similar tools for delamination characterisation are still not available. Without a better understanding of progressive failure, the fracture criteria and predictive capabilities will be limited. Delamination is one of the predominant forms of failure in laminated composites due to the lack of reinforcement in the thickness direction. The analysis of delamination is commonly divided into the study of initiation and the monitoring of the propagation of an already initiated defect. Crack propagation is usually predicted using the Fracture Mechanics approach which eliminates the difficulties associated with the stress singularity at the crack front, but requires the presence of a pre-existing delamination whose exact location may be difficult to determine in real applications. It is also essential to develop computational methods for the simulation of the delamination growth and the interlaminar damage mechanisms. In order to do this it is important to carefully observe and understand the fracture processes to be simulated.

The purpose of this research is to analyze the phenomenon of delamination in sandwich specimens with a rigid core (polyurethane foam), to observe the interlaminar damages and failures, and to try to understand most of the local processes. We continue the using of digital image correlation (DIC) for establishing the three-dimensional displacements of the tested composites and for monitoring the crack propagation [1, 2]. Clearly phenomena are non-linear, and the concept of critical energy release rate used within linear elastic fracture mechanics is doubtful within this context. The use of digital correlation method gave new perspectives in the evaluation of local parameters suitable for damage characterization and interlaminar failure. We proposed as a failure parameter the local strain at the crack tip established exactly before the stable crack propagation occurs, which was in our tests 17.5 % (mean value). Of course that such a parameter is specimen and loading dependent, but, however, it can be established for each situation. An alternative parameter can be the crack tip opening displacement (CTOD) which has an average value of 0.24 mm, when crack propagation occurs. Further developments were obtained by using numerical simulations and cohesive finite elements.

Present work concentrates on the issue of interface failure in a sandwich component with a glass fibre skin and a rigid polyurethane core. Digital image correlation is used in monitoring the evolution of failure from an initial interface crack by using two rows of virtually emulated strain gages of 1.4 mm at the

interface and beneath the interface. Their number for each test depends on the way in which the crack propagated. In this way many information on strain evolution and localization are acquired.

## 2. Theoretical formulation of the interface crack problem

A crack at the common interface or parallel to the interface of two materials with different elastic constants can be encountered in many practical situations, therefore establishing the stress and strain fields around the crack tip as well as the propagation of the crack are of real interest. The interface itself can have a high toughness, which complicates the occurring problems. If the interface between the two different media is of low toughness crack propagation will be produced in a mixed mode and not in mode I, as it happens in a homogeneous and isotropic body. The asymmetry of the moduli of elasticity and the possible unsymmetrical loading will lead to the existence of mode II. Complicated local mechanisms may appear, in between the propagation of the crack along the interface and the deviation of its path through a rapid change of direction, different behaviours being given by the relative toughnesses of the two materials in contact. The classical mathematical formulations of these problems were established as follows. Williams [3], Sih and Rice [4], Rice and Sih [5] used functions of complex variable and series expansions, and Erdogan [6, 7] solved the problem with the help of Hilbert spaces. Bahar [8] introduced a technique of integral transformations. Williams [3] had the merit of first showing the oscillatory character of the stresses proportional to  $r^{-1/2}(\sin)$  or  $(\cos)$  of the argument  $(\varepsilon \log r)$ , where  $r$  is the distance measured from the crack tip and  $\varepsilon$  depends on the elastic constants of the materials. His solution hasn't defined quantitatively the stress fields, but has presented qualitatively the problems which appear. Bahar [8] showed that the stresses don't have an oscillatory character and his solution is questionable. We have to underline some of the papers written by Hutchinson and co-workers [9, 10, 11] which not only brought significant clarifications of the problems, but also studied in detail the case of the cracks parallel to the interface. This problem was also discussed in [12].

Two linear elastic and isotropic materials are divided by an interface and a crack along it (Fig. 1). Let's consider the materials #1 (top) and #2 (bottom) having at the crack tip a cartesian  $(x,y)$  system or a polar one  $(r,\theta)$ , with different elastic constants  $G_i$ ,  $E_i$ ,  $\nu_i$ , ( $i = 1,2$ ) as: transversal modulus of elasticity, longitudinal modulus of elasticity, respectively Poisson's ratio. The following notation is further used:  $k_i = 3 - 4\nu_i$  for state of plane strain and  $k_i = (3 - \nu_i)/(1 + \nu_i)$  for state of plane stress.

Dundurs [13] showed that in the presence of two different materials two important parameters which depend on the elastic constants can be calculated as:

$$\alpha = \frac{G_1(k_2 + 1) - G_2(k_1 + 1)}{G_1(k_2 + 1) + G_2(k_1 + 1)} \quad \text{and} \quad \beta = \frac{G_1(k_2 - 1) - G_2(k_1 - 1)}{G_1(k_2 + 1) + G_2(k_1 + 1)} . \quad (1)$$

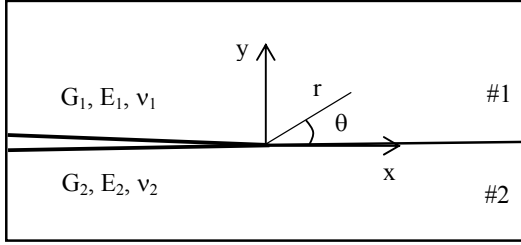


Fig. 1. Notation of the interface constants.

A more suggestive form for  $\alpha$  is

$$\alpha = (\bar{E}_1 - \bar{E}_2) / (\bar{E}_1 + \bar{E}_2) , \quad (2)$$

where  $\bar{E}_i = E_i / (1 - \nu_i^2)$  for plane strain and  $\bar{E}_i = E_i$  for plane stress. Parameters  $\alpha$  and  $\beta$  become zero if it is only one material. The value of the parameter  $\alpha$  reaches +1 if material #1 is more rigid than material #2, and -1 when material #1 is more deformable (compliant) than #2.

For plane strain the parameter  $\beta$  becomes zero when both materials are incompressible ( $\nu_1 = \nu_2 = 0.5$ ). For plane stress,  $\beta = \alpha/3$  when  $\nu_1 = \nu_2 = 1/3$ . When  $\nu_1 = \nu_2$  parameter  $\alpha$  is the same for plane stress or plane strain.

The difference between the elastic constants of the two materials produces an oscillatory stress field [3], proportional to the trigonometric functions (sin) or (cos) of the form  $\sigma \sim (\sin, \cos)(\varepsilon \log r)$ , where  $r$  is the radius measured from the crack tip till the considered point, and  $\varepsilon$  is a so-called oscillatory index defined as

$$\varepsilon = \frac{1}{2\pi} \ln \left( \frac{G_1 + k_1 G_2}{k_2 G_1 + G_2} \right) = \frac{1}{2\pi} \ln \left( \frac{1 - \beta}{1 + \beta} \right) . \quad (3)$$

At the tip of the interface crack in between two semi-spaces, a complex stress intensity factor  $K = K_1 + iK_2$  results, with a real part  $K_1$  (measure of the singularity of the normal stresses) and an imaginary part  $K_2$  (connected to the

singularity of the shear stresses), being connected to the conventional values belonging to mode I and mode II.

The relations which calculate the stresses become complicated, but for  $r \rightarrow 0$  and  $\theta = 0$  they have the simpler form[9]:

$$\sigma_y + i\tau_{xy} \rightarrow \frac{Kr^{i\varepsilon}}{\sqrt{2\pi r}} \quad (4)$$

with  $r^{i\varepsilon} = \cos(\varepsilon \ln r) + i \sin(\varepsilon \ln r)$ . All these lead to a so-called *oscillatory singularity* of the stresses which does not appear in LEFM. The singular stress field ahead the interface crack is given by the relations:

$$\sigma_y = \operatorname{Re}[Kr^{i\varepsilon}] (2\pi r)^{-1/2}, \quad \tau_{xy} = \operatorname{Im}[Kr^{i\varepsilon}] (2\pi r)^{-1/2}. \quad (5)$$

If a crack of length  $2a$  is located at the interface of two semi-infinite materials loaded by  $\sigma_y^\infty$  and  $\tau_{xy}^\infty$ , then at the right tip of the crack one obtains

$$K_1 + iK_2 = (\sigma_y^\infty + i\tau_{xy}^\infty) (1 + 2i\varepsilon) (\pi a)^{1/2} (2a)^{-i\varepsilon}. \quad (6)$$

These stress intensity factors (SIFs) are influenced by the dimensions of the studied body, by the interaction between the crack and the loading, as well as by the interaction between the crack and the boundary of the body.

### 3. Tensile testing of the skin and core

All presented tests were reported by Miron in [14]. The tested sandwich composite has skins made from mat with a weight of 300 g/m<sup>2</sup> and a core with density of 200 kg/m<sup>3</sup>. The skins and the core are glued together by a bicomponent polyurethane adhesive. Traction testing of both skin and core are done on a LLOYD LRX PLUS testing machine with the NEXYGEN software at a speed of loading of 3 mm/min. An extensometer Epsilon with a gage of 50 mm was also used to measure strains. On the other hand, digital image correlation (DIC) with the ARAMIS 2M system were used to monitor strains on the tested specimens. A calibre of 25 x 38 mm was used. One frame per second was acquired.

#### Testing of the skin

Specimens of about 20 mm width and 1.5 mm thickness were tested (Fig. 2). Five tests were done and each time, in order to calculate also Poisson's ratio, two virtual strain gages of 15 mm were emulated in the middle of the specimen: one longitudinal and the other transversal (Fig. 2). In figure 3 longitudinal strains

before failure are shown in the skin as being localized around glass fibres which break. Initial failure of the mat fibres start at about 60 MPa and nonlinearities in the stress-strain diagram appear.

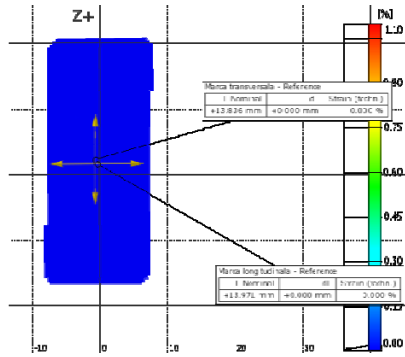


Fig. 2. Skin with virtual strain gages used in ARAMIS.

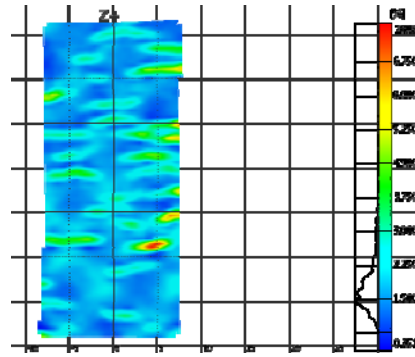


Fig. 3. Longitudinal strains in the skin before failure.

The obtained results for the five tests are given in table 1.

**Experimental results for the traction of the glass fibre mat skin**

*Table 1*

Specimen No.	Dimensions		Established properties			
	Width [mm]	Thickness [mm]	Ultimate stress [ MPa ]	Maximum strain at failure [ % ]	Longitudinal modulus [ MPa ]	Poisson's ratio [ - ]
1	19.10	1.98	84.27	1.055	8743.31	0.324
2	16.90	1.65	109.62	1.417	8401.74	0.335
3	18.30	1.88	105.98	1.153	10176.47	0.339
4	18.10	1.60	92.90	1.094	9518.89	0.327
5	16.51	1.59	137.35	1.916	8173.64	0.329

For further calculations we considered, in average, maximum (ultimate) strength as 106 MPa, elongation at failure of 1.33 %, longitudinal (Young's) modulus as 9000 MPa, and Poisson's ratio as 0.33.

### Testing of the core

Same procedure as before was used for the tensile testing of the polyurethane core with a density of  $200 \text{ kg/m}^3$ . The response of the material is nonlinear and more ductile after a stress of 3.5 MPa is reached, and failure is produced around 5.9 MPa. The level of strains is quite low, and no specific indication is noticed before breaking. Just as an example for one test, the

longitudinal strains are shown in the linear elastic domain at a stress of 0.9 MPa (Fig. 4), and in the last frame before failure at 5.98 MPa (Fig. 5).

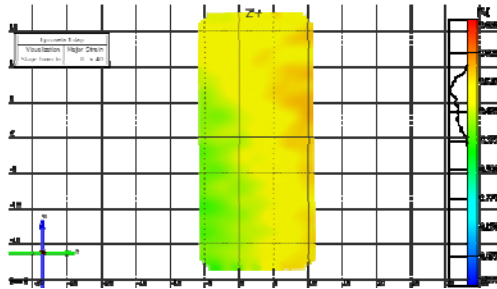


Fig. 4. Longitudinal strains at 0.9 MPa.

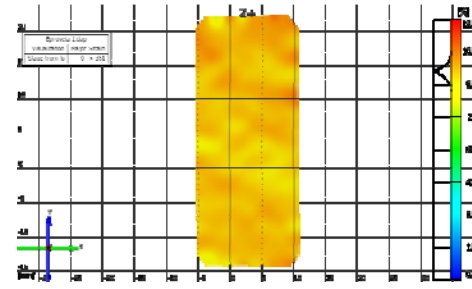


Fig. 5. Longitudinal strains at 5.98 MPa.

Results of two tests are given hereby, in table 2. As seen in figure 5, before the failure of the specimen no indication of the local strain increase in a specific section was noticed.

*Table 2*  
**Experimental results for the traction of the polyurethane core with density 200 kg/m<sup>3</sup>**

Specimen No.	Dimensions		Established properties			
	Width [mm]	Thickness [mm]	Ultimate stress [ MPa ]	Maximum strain at failure [ % ]	Longitudinal modulus [ MPa ]	Poisson's ratio [ - ]
1	19.70	6.55	5.980	12.370	172.059	0.366
2	19.76	6.89	5.940	11.890	172.077	0.374

In average, maximum (ultimate) strength is 5.96 MPa, elongation at failure of 12.13 %, longitudinal (Young's) modulus as 172.1 MPa, and Poisson's ratio as 0.37.

#### 4. Setup of the experiment

The sandwich has the skins with different average thicknesses: top of 1.73 mm, and bottom of 1.98 mm. The polyurethane core is about 12.5 mm. An initial delamination of about 45 mm is produced by introducing a non-adherent film at one of the interfaces. In order to be able to load the specimen, two special tabs of 25 mm are glued on the top and bottom of the specimen towards the end with the insert. The whole specimen is painted in white and black speckle dots in order to be able to use DIC. The specimen prepared for testing is shown in figure 6.

The testing of the sandwich specimen in mode I is done in order to establish the opening strain at the initiation of the degradation and the evolution of the opening strain during crack propagation. On the other hand, the crack opening when damage is completed, before failure is produced at the interface, is also monitored.



Fig. 6. Sandwich composite specimen prepared for testing.

Six specimens were tested till the final failure. Length of the initial delamination is measured and the monitored points during testing are mentioned in table 3.

*Table 3*  
**Dimensions of the tested sandwich specimens and the position of the monitored points**

Specimen No.	Dimensions		Monitored position					
	Width [ mm ]	Thickness [ mm ]	Length of initial delamination [ mm ]	Position of the monitored points [ mm ]				
1	19.8	16.9	46.92	51.98	56.88	61.97	66.91	69.39
2	20.0	16.9	47.05	52.44	59.95	77.40		
3	20.1	17.0	45.17	62.44	73.16			
4	20.3	16.5	53.36	Crack propagates once in the visual field of ARAMIS				
5	20.1	16.9	46.54	51.54	58.44	63.47	69.88	
6	20.3	16.5	43.02	49.91	63.29			

## 5. Results on the interface failure

Speed of loading is also 3 mm/min, and the same calibre 25 x 38 mm is used. Due to the asymmetric position of the interface crack in the specimen (only

one interface has an initial delamination) the specimens have also a rotation while the test is completed. In some tests, the crack propagated with a pop-in. If the interface crack propagates too much it may get out the monitored field by the ARAMIS system which is about the same size as the used calibre. Therefore, not for all tests we obtained the same amount of data.

The analysis of local strain fields around the tip of the initial delamination and after crack propagation is done by using DIC and virtual strain gages of about 1.4 mm. They are positioned normal to the interface and the following notation is used: *I* strain gage is at the interface with the top tip on the lower part of the skin and the bottom tip on the core; *S* strain gage is positioned beneath the *I* strain gage having its top tip common with the bottom *I*-tip and the bottom tip in a lower position in the core (Fig. 7). We are going to call: the *I* strain gage as being interface, and the *S* strain gage as being core.

Strain gages *I* and *S* are in the same location for one monitored point, that is we measure the strains at the interface and in the core. For test 1 there are five positions which are monitored during the failure of the interface crack. In table 4 the initial monitored point is at the tip of the initial delamination. Only strains measured with the *I* gages are given.

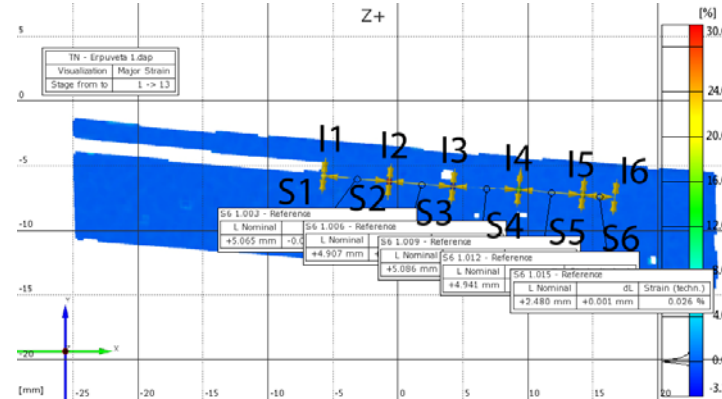


Fig. 7. Position of virtual strain gages along the interface for test 1.

The position of the monitored point indicates the distance towards the edge of the specimen. Gage length of the virtual strain gage  $l_0$  is indicated in table 4 as the exact values of the *I* gages in that particular location; some differences appear with respect to the reference value of 1.4 mm. The frame number is also stated when the initial and final parameters of damage are established. Theoretically, one frame is taken at one second. However, it has been noticed that this is not always true, that is we cannot convert difference in the numbers of frames into time elapsed between initial and final damage.

Table 4

**Behaviour of the interface zone. Strain and opening of the crack**

Test no.	Monitored point (crack tip)			Initial parameters of damage			Final parameters of damage		
	Nr.	Strain gage position	Gage length ( $l_0$ )	Frame	Strain	Crack opening ( $\Delta l$ )	Frame	Strain	Crack opening ( $\Delta l$ )
		[ mm ]	[ mm ]	[ - ]	[ % ]	[ mm ]	[ - ]	[ % ]	[ mm ]
1	1	46.92	1.40	128	8.72	0.122	208	30.28	0.432
	2	51.98	1.40	251	6.67	0.093	269	24.80	0.347
	3	56.88	1.40	305	6.55	0.092	330	28.66	0.402
	4	61.97	1.76	375	8.70	0.153	394	32.45	0.57
	5	66.91	1.40	417	5.00	0.07	458	26.00	0.364
	6	69.39	1.40	468	5.41	0.076	495	32.47	0.455
2	1	47.05	1.38	134	9.63	0.133	166	32.78	0.451
	2	52.44	1.38	176	7.06	0.097	208	32.32	0.445
	3	59.95	1.41	270	9.40	0.132	Unstable propagation; parameters cannot be established		
	4	77.4	1.41	310	10.50	0.149	488	29.48	0.415
3	1	45.17	1.41	96	11.11	0.156	148	27.50	0.387
	2	62.44	1.57	295	10.36	0.163	325	37.10	0.583
	3	73.16	1.59	401	7.12	0.113	439	24.20	0.386
4	1	53.36	1.39	154	6.70	0.093	235	18.08	0.251
5	1	46.54	1.43	111	4.60	0.0658	176	39.90	0.572
	2	51.54	1.41	179	4.69	0.0662	215	34.22	0.483
	3	58.44	1.40	264	5.91	0.083	284	16.47	0.231
	4	63.47	1.40	327	9.82	0.137	353	20.50	0.286
	5	69.88	1.38	421	13.41	0.185	427	25.17	0.348
6	1	43.02	1.43	67	8.27	0.119	151	34.17	0.49
	2	49.91	1.43	202	6.70	0.096	213	14.06	0.201
	3	63.29	1.42	304	7.34	0.104	350	32.64	0.463

For test 1, measurements done before and after the second crack propagation are shown (Fig. 8). The initial and final damage parameters (listed in table 4) are quantified in corresponding frames by using DIC.

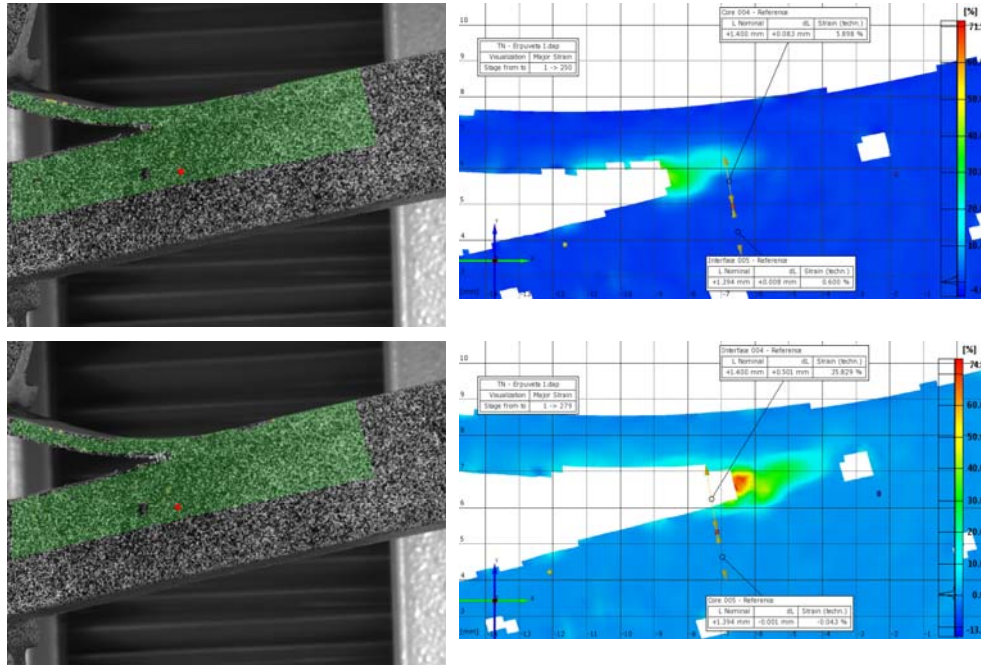


Fig. 8. Picture of the specimen from test 1 and DIC analyses before and after the second crack propagation.

The initial and final parameters of damage are given by the opening strain and relative displacement of the crack flanks – crack opening; these are measured with the locally emulated strain gage and directly with the ARAMIS system. It was tried to keep a distance of about 5 mm in between two consecutive monitored points. This was not always possible as we were interested to establish exactly the position on the specimen in which damage was finalized, that is there was no material in that location. The last analyzed point for each test was chosen as close as possible to the crack position at the end of the analysis.

The moment of damage initiation was chosen as the one at which we obtain the maximum tensile strain in the core of the sandwich, measured with virtual strain gage  $S$ . After attaining this maximum, the material of the core relaxes, and the damage is considered as finalized. Meanwhile, we measure significant local strains at the interface and failure is produced by the crack propagation. When strain in core diminishes, the tip of the crack moves beyond the monitored point.

In Fig. 9 is presented the typical variation of strains in the interface in a monitored point which is initially further away from the tip of the initial delamination [14]. For the second crack propagation the damage processes are

produced in between frames 305 and 350 (Table 4). There are four distinctive domains of strain variations which are obtained:

- *domain I* in which the interface and the core are in compression due to the loading of the specimen; meanwhile the crack propagates in a stable manner towards the monitored point;
- *domain II* in which both interface and core are loaded in tension; the tip of the crack reaches the monitored point;
- *domain III* while damage is produced with increasing strains in the interface and relaxation of strains in the core;
- *domain IV* registers the strains in the material of the core; meanwhile the crack exceeds the point of measurement and, although strains in interface still increase there is no physical significance for such a trend as there is no material left at the interface.

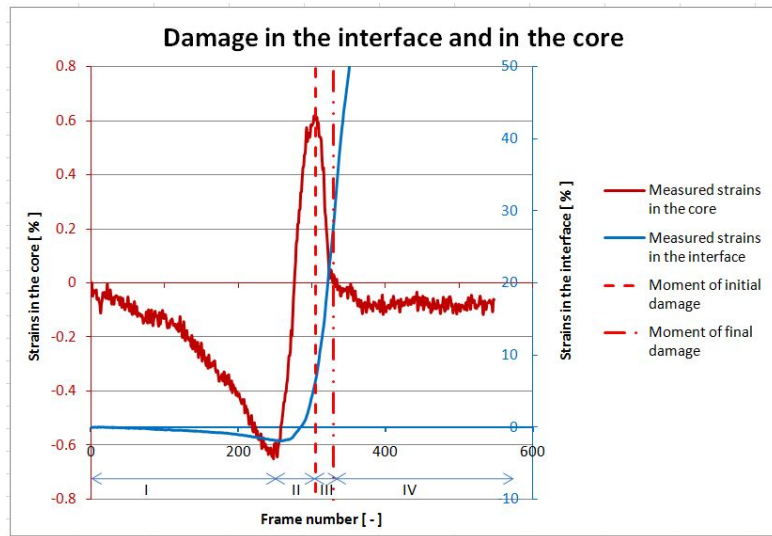


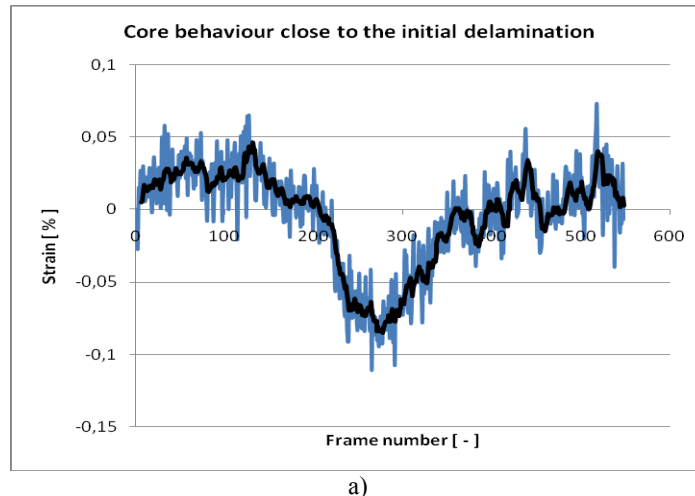
Fig. 9. Variation of strains at the interface and in the core in a monitored point while damage is produced.

After the initiation of damage in the interface the material around the tip of the crack (core) relaxes and strains diminish; meanwhile strains in interface increase significantly. The final (complete) damage of the interface zone is attained when the material of the core relaxes completely and strains remain mostly constant, as seen in figure 9 (domain IV).

Three distinct strain responses can be identified by analyzing the strain evolution that occurs in the core of the sandwich material, close to the interface region. Figure 10 a) shows the evolution of the strain recorded in the core, at the

position of the initial crack tip. Local traction strains are recorded for the first part of the experiment, followed by a relaxation zone. The strains that are recorded in the core, at the initial crack tip position are relatively small causing a high amount of noise in the results obtained using DIC method. The resolution of the ARAMIS 2M system is in the vicinity of strain 0.05 % level obtained for this monitored position (measuring range is from 0.01 % and the strain accuracy is up to 0.01 %). The main solution to avoid noise obtained during analysis is to use a smaller sized calibre but this will also reduce the size of the analyzed area; such a decision is not desirable because the results are affected by the rigid body motion of the tested specimen during the experiment. In the same time, a smaller area of analysis allows the study of a smaller interface length, and in the case of unstable crack propagation growth the crack tip will leave the area of analysis.

A second type of core behaviour is noted as being typical for measuring points positioned between 5 and 12 mm from the crack tip, represented graphically in figure 10 b). First, the core close to the interface layer suffers a local compression which lasts until the crack tip advances to its vicinity. The local compression stage is followed by a local tensile strain that will last until the interface damage initialization. The moment of interface damage initialization is marked by the maximum value of the strain recorded in the core. During damage development the core gradually relaxes marking the end of the damage process. The complete failure of the interface corresponds to the end of the relaxation in the core.



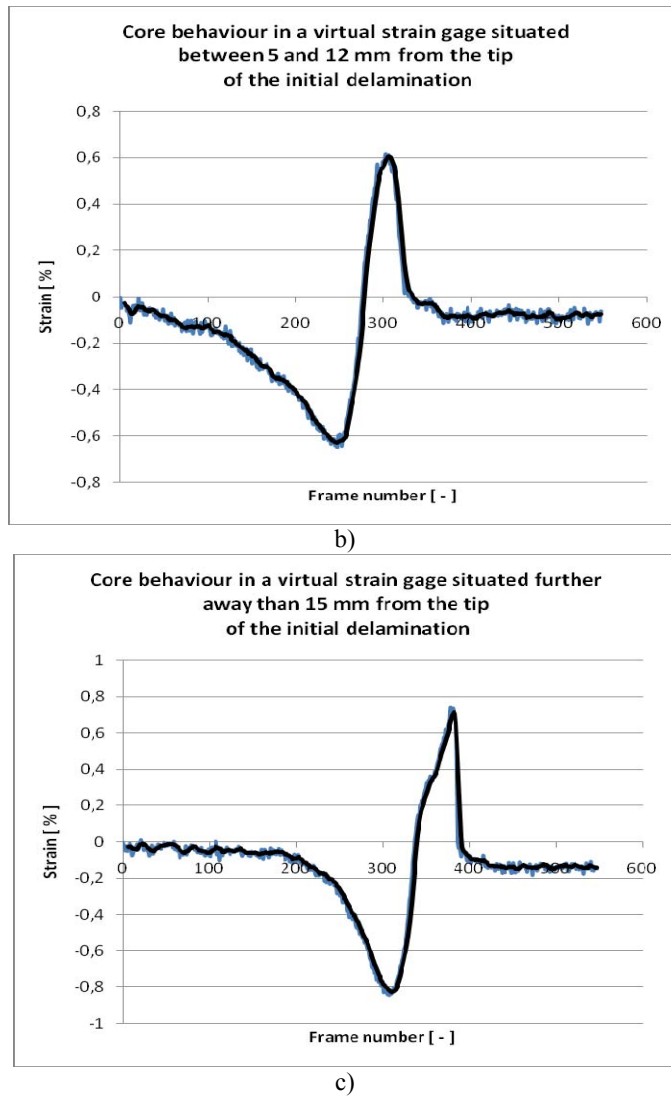


Fig. 10. Strain evolution in the core at different distances from the initial delamination:  
 a) strains at the initial delamination; b) strains in between 5 to 12 mm from the crack tip; c) strains at distances greater than 15 mm from the crack tip.

The third type of strain localization is similar to that described above, the only difference consists in the presence, at the beginning of the test, of a zone in which no loading of the core is recorded (Fig. 10 c)). This is because the measuring point is located far enough from the initial crack tip. As the crack steadily propagates towards the measuring position, the material behaves similar to the previous description. This type of behaviour was found for all the

measuring points placed at a distance greater than 15 mm from the initial crack tip.

## 6. Comment on the interface parameters

Coming back to the calculus of interface parameters  $\alpha$  and  $\beta$  established by Dundurs, in our case we can consider material #1 as being the glass fibre mat skin with  $E_1 = 9000$  MPa and  $v_1 = 0.33$ , and material #2 the polyurethane core with  $E_2 = 172.1$  MPa and  $v_2 = 0.37$ . State of plane stress is considered. Therefore  $k_1 = 2.007$  and  $k_2 = 1.9197$ . By using relation (2) it results  $\alpha = 0.9625$ , and from (1)  $\beta = 0.3028$ . By using equation (3) the value of the oscillatory index becomes  $\varepsilon = -0.1$ . Another important interface parameter was established by Hutchinson et al. [9] who made an energetic equivalence between the complex generalized SIF notated  $K = K_1 + iK_2$ , and the classical ones notated  $K_I$  and  $K_{II}$  (for modes I and II) through the relation

$$K_I^2 + K_{II}^2 = q^2 K \bar{K} \quad (7)$$

in which  $\bar{K}$  is the conjugated of the complex SIF  $K$ . In our situation  $q = 0.68$ .

It comes out that mode II is also present in our particular case of the interface problem for the sandwich specimen. We can evaluate for the moment - from the experimental measured displacement fields - that mode II is about 10 % out of mode I. Further analyses will elaborate on this issue.

## 7. Conclusions

The issue of interface failure in a sandwich component with a glass fibber skin and a rigid polyurethane core is analyzed by using the digital image correlation method. Virtual strain gages are emulated at the interface and beneath it, in the material of the core. The moment of damage initiation and its evolution are monitored by measuring the local opening strain with the ARAMIS system. Several monitored points assess crack propagation and the response of the skin and of the core when failure is finalized. Crack opening can be also measured when failure is completed.

Four main domains are encountered and comments in figure 9 are done concerning their characteristics. Mixed modes are present at the interface and their analyses are going to be done elsewhere.

Strain localization in front of the initial delamination shows different patterns, as illustrated in figure 10, depending on the relative distance from the tip. When comparing figures 10 c) to 10 b) the compression strains in the core disappear, as we are further away from the delamination tip. However, the maximum positive strains are about the same, as 0.6-0.7 %, showing an imminent

delamination failure. The strain localization phenomena enlarge the perspectives of the analyses on successive failures at the interface during the same test. All these phenomena are essentially nonlinear and the proposed procedure gives a more realistic perspective on the evaluation of interlaminar damage.

### Acknowledgements

The research done by the PhD student eng. Matei Constantin Miron has been funded by the Sectoral Operational Programme **Human Resources Development** 2007-2013 of the **Romanian Ministry of Labour, Family and Social Protection** through the Financial Agreement POSDRU/6/1.5/S/19.

### R E F E R E N C E S

- [1] *D.M. Constantinescu, M.C. Miron, and D.A. Apostol*, “Evaluation of interlaminar damage and crack propagation in sandwich composites”, in *Lucrările celui de-al XIV-lea Simpozion Internațional de Mecanica Ruperii*, 10-11 octombrie, Brașov, ISSN 1453-6536, 2008, pp. 3-9
- [2] *M.C. Miron, D.A. Apostol and D.M. Constantinescu*, “Interactions of neighbouring delaminations in a sandwich composite”, in *Lucrările celui de-al XV-lea Simpozion Național de Mecanica Ruperii*, 6-7 noiembrie, Sibiu, ISSN 1453-6536, 2009, pp. 1-8
- [3] *M.L. Williams*, “The Stresses Around a Fault or Crack in Dissimilar Media”, in *Bulletin of the Seismological Society of America*, **vol. 49**, 1959, pp. 199-204
- [4] *G.C. Sih, J.R. Rice*, “The Bending of Plates of Dissimilar Materials With Cracks”, in *Journal of Applied Mechanics*, **vol. 31**, pp. 477-482, 1964.
- [5] *J.R. Rice, G.C. Sih*, “Plane Problems of Cracks in Dissimilar Media”, *Journal of Applied Mechanics*, **vol. 32**, 1965, pp. 418-432
- [6] *F. Erdogan*, “Stress Distribution in a Nonhomogeneous Elastic Plane With Cracks”, *Journal of Applied Mechanics*, **vol. 30**, 1963, pp. 232-236
- [7] *F. Erdogan*, “Stress Distribution in Bonded Dissimilar Materials with Cracks”, *Journal of Applied Mechanics*, **vol. 32**, 1965, pp. 403-410
- [8] *L.Y. Bahar*, On an Elastostatic problem in Nonhomogeneous Media Leading to Coupled Dual Integral Equations, PhD dissertation, Lehigh University, Bethlehem, Pa., 1963
- [9] *J.W. Hutchinson, M.E. Mear and J.R. Rice*, “Crack Paralleling an Interface Between Dissimilar Media”, *Journal of Applied Mechanics*, **vol. 54**, 1987, pp. 828-832
- [10] *Z. Suo, J.W. Hutchinson*, “Interface Crack between Two Elastic Layers”, *International Journal of Fracture*, **vol. 43**, 1990, pp. 1-8
- [11] *J.W. Hutchinson, Z. Suo*, “Mixed Mode Cracking in Layered Materials”, in *Advances in Applied Mechanics*, **vol. 29**, 1992, pp. 63-91
- [12] *C.W. Smith, K.T. Gloss, D.M. Constantinescu and C.T. Liu*, “Stress Intensity Factors for Cracks Within and Near to Bondlines in Soft Incompressible Materials”, in *Recent Advances in Solids and Structures*, ASME, **PVP.-vol. 415**, 2000, pp. 1-9
- [13] *J. Dundurs*, *Mathematical Theory of Dislocations*, ASME, New York, 1969
- [14] *M.C. Miron*, Analiza propagării fisurilor interlaminare în componete de tip sandwich (Analysis of interlaminar crack propagation in sandwich composites), Master in Engineering dissertation, University POLITEHNICA of Bucharest, 2010 (in Romanian)